

Electrodeposited CoNiP Coating on 42CrMo Steel as Gear Material and its Wear Resistance Performance in Simulated Oil

Zhang Huicheng^{1,2}, Wang Yufeng¹, Li Yujun¹

¹ Undergraduate Teaching Department, Jiuquan Vocational Technical College, Jiuquan 735000, China

² School of Mechanical and Electronical Engineering, Lanzhou University of Technology, Lanzhou 730050, China

*E-mail: zhanghc_vtc@yeah.net

Received: 4 March 2022 / Accepted: 25 March 2022 / Published: 7 May 2022

Different CoNiP alloy coatings were electrodeposited from plating solutions with various concentrations of sodium hypophosphite on the surface of 42CrMo steel plate as gear material to improve mechanical performance in simulated oil. CoNiP alloy coating presents granular morphology with crystalline structure. Sodium hypophosphate in plating solution is beneficial to accelerate the chemical reaction rate, increase the thickness of the coating and refine the surface particles, so as to improve the wear resistance. However, when the content of sodium hypophosphite is higher than 15 g/L, the stability of the bath decreases to obtain coatings with loose and rough structures, resulting in the decrease of wear resistance. The CoNiP alloy film prepared at 15 g/L sodium hypophosphite has the best crystallinity, compact surface and excellent wear resistance.

Keywords: Electrodeposition; CoNiP alloy coating; Wear resistance; Gear materials; Simulated oil;

1. INTRODUCTION

Gear parts are widely used in modern manufacturing, which are considered as critical and core components due to their optimal advantages, such as precision, stability, high efficiency and so on [1-4]. Along with the development of science and technology, gear is indispensable in various fields. For example, traditional machine tools are equipped with a large number of gear parts. As the basic equipment of manufacturing industry, machine tool directly determines the quality of mechanical products. The gear device is also widely used in the automobile industry. The gear is one of the key devices to realize the power transmission and speed control of the automobile, which directly affects the power system and service life of the vehicle.

Steel is one of the commonly used materials for gear. At present, the steel commonly used in gear is tempered steel, hardened steel, nitriding steel and so on [5-10]. Wear resistance performance is

an important parameter for gear material. In order to further improve the mechanical performance of gear materials, it is useful to prepare alloy coatings with better mechanical performance on the surface of gear material. For example, some alloy coatings such as CoW, FeNi, NiW and ZnNi are fabricated to improve physical and chemical performance of substrate reported in many literatures [11-15]. In addition to alloy coatings, it is found that some nano-particles or non-metals are also beneficial to improve performance of materials [16-20].

42CrMo steel possesses good mechanical performance and optimal machinability which is widely used as gear materials. According to previous research by others, phosphorus has strong solution strengthening effect, which increases the strength and hardness of metal materials [21-24]. However, many works focus on the effect of phosphorus on electroless plating, attributed to sodium hypophosphite mainly as a reducing agent in electroless plating. Therefore, in the paper, sodium hypophosphite was introduced during plating process to prepare CoNiP alloy coatings on the surface of 42CrMo steel as gear material. Moreover, the wear resistance of CoNiP alloy coatings in simulated oil was also studied.

2. EXPERIMENTAL

2.1 Materials and technical process

42CrMo steel plate, a typical gear material, was used as the substrate (20 mm×40 mm×1 mm) in the plating process.

Table 1. Plating solution and technology parameter of CoNiP coating

Chemical agent and parameter	Value
CoSO ₄ ·7H ₂ O	30 g/L
NiSO ₄ ·6H ₂ O	30 g/L
C ₆ H ₅ Na ₃ O ₇	80 g/L
Na ₂ SO ₄	20 g/L
H ₃ BO ₃	30 g/L
NaH ₂ PO ₂ ·6H ₂ O	0~20 g/L
Current density	2.5 A/dm ²
Plating time	1 hour
Temperature	60 °C

The chemical component of 42CrMo is: 0.38-0.45% C, 0.17~0.37% Si, 0.5-0.8% Mn, 0.9-1.2% Cr, 0.15-0.25% Mo, the rest part is Fe. The pure platinum plate (40 mm×40 mm×1 mm) was chosen as the counter electrode. The substrate was polished and cleaned sequentially. After that, the substrate was immersed into an alkaline solution (20 g/L NaOH, 18 g/L Na₂CO₃ and 10 g/L Na₃PO₄) to get rid of oils at 60 °C for 15 minutes. And then, 10% hydrochloric acid was used to do rust cleaning for the substrate. Finally, the substrate was cleaned and dried to do the CoNiP electrodeposition in 200 ml

plating solution at 60 °C for 1 hour. The specific information of plating solution and technology parameters is listed in Table 1.

2.1 Simulated oil solution

Gears work in oil to extend their service life and improve transmission efficiency. The oil is composed of based lubricating oil and compound additives. In the paper, wear resistance of CoNiP alloy coating electrodeposited on surface of 42CrMo steel in simulated oil was investigated. The composition of simulated oil is listed in Table 2.

Table 2. Composition of simulated oil solution

Chemical agent	Mass percent/ %
Based oil 400SN	70%
Sodium sulfite	5%
Sodium dodecyl benzene carbonate	10%
Potassium metabo	8%
Oleamide	7%

2.3 Performance testing

The chemical station CHI440C was used to study electrochemical mechanism of CoNiP electrodeposition based on cyclic voltammetry and i-t curves. During the cyclic voltammetry testing and i-t curves, the anode was pure platinum plate (40 mm×40 mm×1 mm) and the cathode was the 42CrMo steel plate (10 mm×10 mm). Saturated calomel electrode was utilized as the reference electrode. The high voltage was 0.1 V while the low voltage was -1.3 V at the scanning rate of 0.01 V/s in the cyclic voltammetry testing. According to the experiment of i-t curves, the voltage was stable at -1.3 V for 250 seconds. The wear resistance of samples in simulated oil was tested by friction abrasion machine (M200). The load force was 10 N to abrade for 20 minutes with 3 mm length wear scratch. The thickness and wear profile were tested by surface profiler (KlaTencor P6). Microstructure of CoNiP coatings was characterized by X-ray diffraction (XRD-7000) while the surface morphology was observed by scanning electron microscope (TM3000).

3. RESULTS AND DISCUSSION

3.1 Cyclic voltammetry curves

The cyclic voltammetry curves of different plating solutions (0.01 M CoSO₄, 0.01 M NiSO₄, 0.01 M NaH₂PO₂, 0.01 M CoSO₄+0.01 M NiSO₄ and 0.01 M CoSO₄+0.01 M NiSO₄+0.01 M NaH₂PO₂) are tested by electrochemical station to investigate the electrodeposition mechanism of CoNiP coatings. The result is shown in Figure 1.

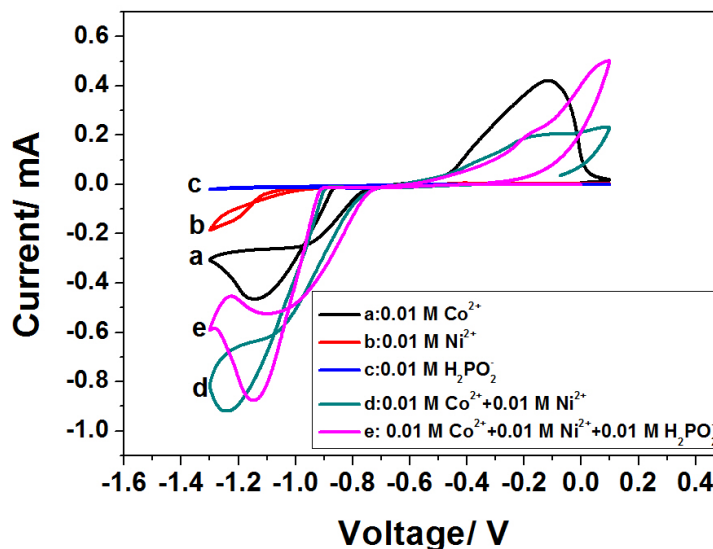
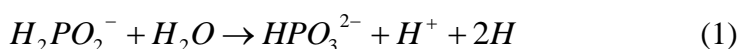


Figure 1. The cyclic voltammetry curves of different plating solutions. The high voltage is 0.1 V while the low voltage is -1.3 V at the scanning rate of 0.01 V/s.

As seen in Figure 1, the reaction current of cobalt increases sharply at the position of -0.866 V that means the deposition of cobalt is dominant. Moreover, a reduction peak of cobalt could be observed at the position of -1.14 V. The diffusion rate of cobalt ions in the solution is slower than that of electrochemical reaction rate. The concentration of cobalt ions at the cathode is substantially lower as the potential shifts to a more negative position, resulting in the appearance of a reduction peak. According to the cyclic voltammetry curve of nickel, the deposition current of nickel starts to increase obviously at the voltage of -0.751 V which is more positive than cobalt. There is no obvious reduction peak found in nickel cyclic voltammetry curve, which is because the electrodeposition of nickel is controlled by electrochemistry. The curve d indicates the electrodeposition of CoNi, the current starts to increase extremely at the position of -0.891 V. When phosphorus is added into the electrolyte, the deposition voltage of CoNiP moves to the position of -0.912 V, which means that electrodeposition of alloys need larger potential. However, the gradient of CoNiP cathode current is larger than Co and CoNi which indicates that the electrodeposition process of CoNiP is accelerated. From the curve of solution with sodium hypophosphite, there is basic no reaction current could be detected. This phenomenon means that phosphorus cannot be electrodeposited from a solution containing only sodium hypophosphite. The deposition mechanism of phosphorus is illustrated by equations below [25-27].



In the electrodeposition of CoNiP alloy coatings, phosphorus is precipitated under the catalytic action of cobalt and nickel. *MH* represents the primary atomic hydrogen adsorbed on the metal surface,

and the primary hydrogen decomposed by hypophosphite is adsorbed on the surface of nickel or cobalt metal. The nickel and cobalt metal can play a catalytic role in the primary hydrogen, thus promoting the precipitation of phosphorus. Phosphorus plays a role in improving corrosion resistance performance of materials, which has been reported in many papers [28-31].

3.2 I-t electrochemical curves

Figure 2 shows the i-t curves of Co, Ni, CoNi and CoNiP electrodeposition at the potential of -1.3 V for 250 s. At the initial stage of electrodeposition, the current increases gradually to a maximum value due to the cobalt or nickel nucleation on the cathode surface resulting in the increase of surface area. As the electrochemical reaction progresses, the thickness of diffusion layer increases and the current decreases to be a constant value (i_c) after the plating system gets an equilibrium state. The peak current (i_m), time of peak current (t_m) and balance current (i_c) are three important parameters which determinate the nucleation mechanism in the early stage of electrochemistry. Instantaneous nucleation and continuous nucleation are two classical nucleation processes [32-33]. Instantaneous nucleation is characterized by the initial electrodeposition on the activation area of the substrate surface. Continuous nucleation requires an induction period, and the nucleation process is related to time. Generally speaking, the nucleation mechanism of cobalt is instantaneous while the nickel belongs to continuous nucleation which has been investigated by some people [34-36].

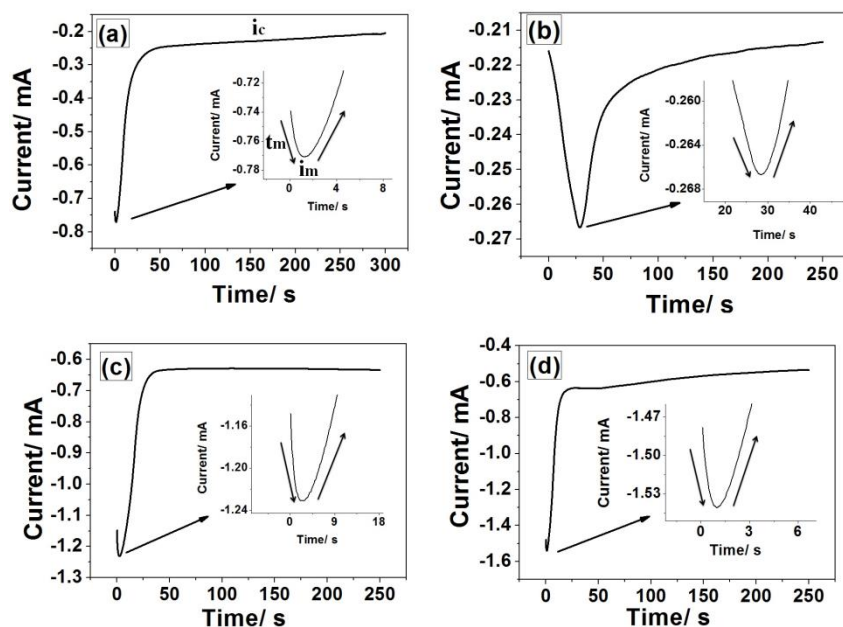


Figure 2. The i-t curves of Co, Ni, CoNi and CoNiP. a:0.01 M CoSO₄; b:0.01 M NiSO₄; c:0.01 M CoSO₄+0.01 M NiSO₄; d: 0.01 M CoSO₄+0.01 M NiSO₄+0.01 M NaH₂PO₂; The applied voltage is -1.3 V for 250 s.

3.3 Thickness of CoNiP alloy coatings

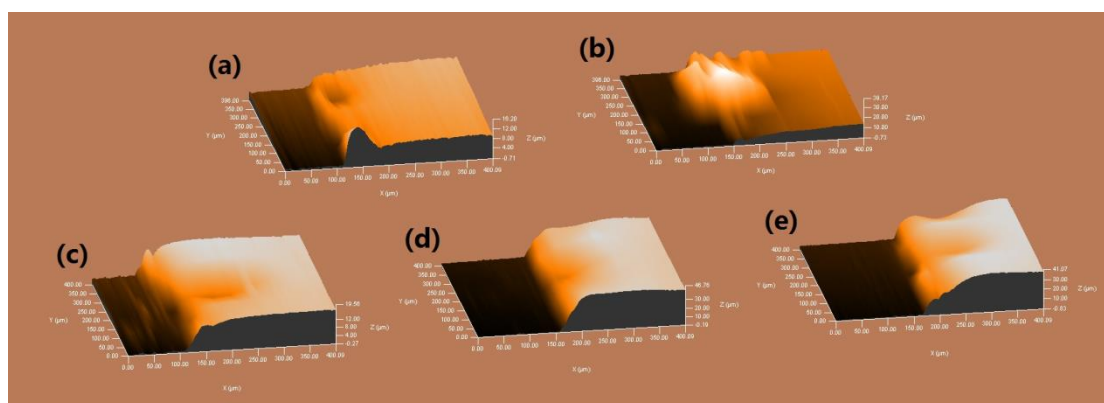


Figure 3. Thickness of CoNiP alloy coatings prepared from solutions with different amounts of sodium hypophosphite; a:0 g/L NaH₂PO₂; b:5 g/L NaH₂PO₂; c:10 g/L NaH₂PO₂; d:15 g/L NaH₂PO₂; e:20 g/L NaH₂PO₂; The scanning area is 400 μm×400 μm at the scanning rate of 10 μm/s.

Table 3. Thickness of CoNiP alloy coatings

Sample	NaH ₂ PO ₂ / g/L	Minimum step height/ μm	Maximum step height/ μm	Average step height/ μm
a	0	-0.71	16.20	8.35
b	5	-0.73	39.17	13.72
c	10	-0.27	19.56	18.23
d	15	-0.19	46.76	35.57
e	20	-0.83	41.07	30.12

Based on the cyclic voltammetry and i-t curves, it is found that adding phosphorous can affect deposition potential and reaction current during plating which is also reported in some works [37-38]. For example, certain amount of phosphorous in the plating bath can affect the morphology and structure of NiP coatings during electrodeposition [39-40].

Therefore, it is significant to study the effect of sodium hypophosphite on physical and chemical performance of CoNiP alloy coatings. The thickness of CoNiP alloy coatings prepared from solutions with different amounts of sodium hypophosphite is shown in Figure 3 and Table 3. It can be seen that, the CoNi alloy coating prepared from solution without sodium hypophosphite has the average thickness of 8.35 μm. The average thickness of CoNiP alloy coating increases steadily from 13.72 μm to 35.57 μm as sodium hypophosphite concentration increases from 5 g/L to 15 g/L. The decomposition of hypophosphite produces atomic hydrogen, which is catalyzed by the surface of nickel and cobalt, thus promoting the precipitation of phosphorus. Moreover, atomic hydrogen is beneficial to accelerate the electrodeposition of nickel and cobalt ions. However, when the sodium hypophosphite is higher than 15 g/L, the average thickness of CoNiP alloy coating decreases due to decomposition of sodium hypophosphite.

3.4 Structure and surface morphology of CoNiP alloy coatings

The structure of CoNiP alloy coatings are investigated by XRD patterns shown in Figure 4. The XRD patterns show obvious crystal structure. Four strong diffraction peaks are observed at 44.5° , 51.5° , 76.2° and 93.2° respectively which indicates the fcc crystal structure of CoNi. Similar structure of CoNi alloys have also been reported by some scholars [41-42]. However, the electrodeposited CoNiP with amorphous and nanocrystalline structure has also been reported due to different electrodeposition parameters [43-44].

According to the Figure 4, fcc structure of Co and Ni are also found. The diffraction intensity of CoNi increases firstly and then decreases with the increase of sodium hypophosphite concentration in the plating solution. This is mainly because proper amount of sodium hypophosphite in the plating solution can accelerate the electrochemical reaction rate of CoNi, increase the thickness and deposition quality, resulting in the improvement of CoNi diffraction intensity. Sodium hypophosphite is a typical reducing agent. Excessive sodium hypophosphite is easy to decompose, which reduces the stability of the bath and decreases the crystallinity of CoNi alloy. Moreover, with the increase of the concentration of sodium hypophosphite in the bath, the diffraction peaks of cobalt and nickel in the XRD pattern also increase significantly. This phenomenon further shows that sodium hypophosphite is beneficial to accelerate the deposition rate of cobalt and nickel.

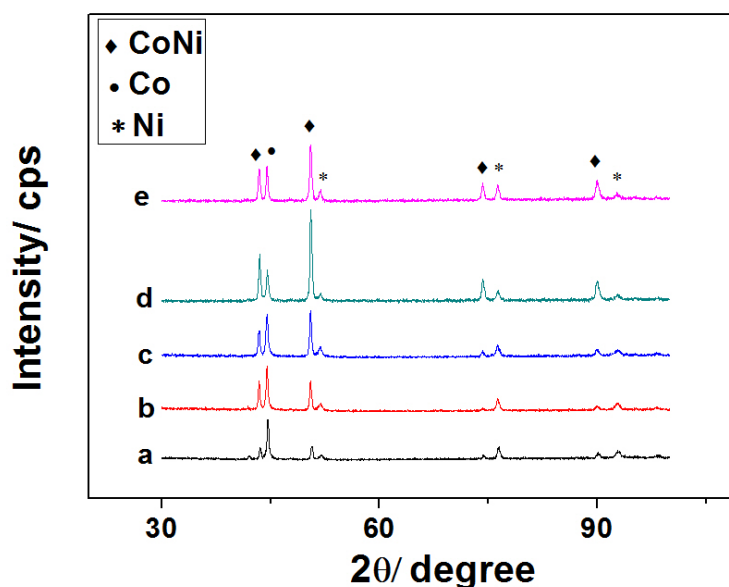


Figure 4. Structure of CoNiP alloy coatings prepared from solutions with different amounts of sodium hypophosphite; a:0 g/L NaH_2PO_2 ; b:5 g/L NaH_2PO_2 ; c:10 g/L NaH_2PO_2 ; d:15 g/L NaH_2PO_2 ; e:20 g/L NaH_2PO_2 ; The scanning angle is from 30° to 100° at the scanning rate of $2^\circ/\text{s}$.

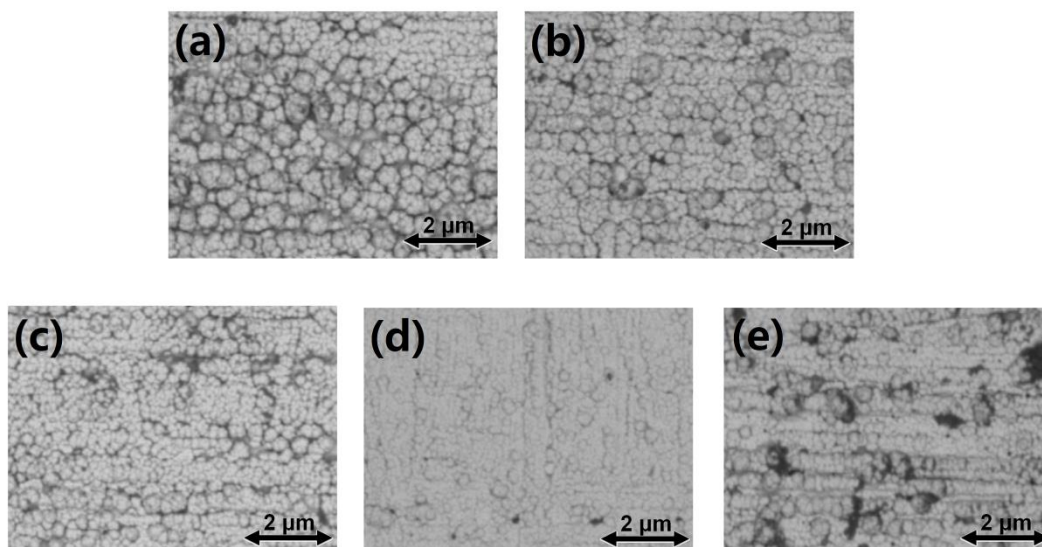


Figure 5. Surface morphology of CoNiP alloy coatings prepared from solutions with different amounts of sodium hypophosphite; a:0 g/L NaH_2PO_2 ; b:5 g/L NaH_2PO_2 ; c:10 g/L NaH_2PO_2 ; d:15 g/L NaH_2PO_2 ; e:20 g/L NaH_2PO_2 ;

Figure 5 demonstrates the surface morphology of electrodeposited CoNiP alloy coatings. CoNiP alloy coating shows a kind of particle morphology, a few particles appear agglomeration phenomenon. When the content of sodium hypophosphite is low, the surface particles of CoNiP alloy are larger and agglomeration is obvious. With the increase of sodium hypophosphite concentration, surface of CoNiP particles become uniform, fine and compact. The main reason is that the high concentration of sodium hypophosphite in the bath increases the content of phosphorus in the coatings. Phosphorus precipitates on the surface of the CoNi alloy coating, which can enter the lattice of the alloy to prevent crystal growth, refine the grain, and form a relatively compact and fine grain structure. However, it is found that when the sodium hypophosphite in the bath is greater than 15 g/L, the coating becomes black and the coating surface becomes loose and rough.

3.5 Wear resistance of CoNiP alloy coatings

The different CoNiP alloy coatings electrodeposited on 42CrMo steel plate as gear material are abraded in the simulate gear oil environment to evaluate the wear resistance performance. After the testing of abrasion, the gear oil on the sample surface is cleaned and the wear scratch profiles are observed and shown in Figure 6. As can be seen from Figure 5, the surface of CoNiP alloy coating presents U-shaped wear scratch morphology after wear testing. The depth and width of the wear scratch of CoNiP alloy coatings prepared from different sodium hypophosphite solutions are quite different. Compared with the CoNiP alloy coating, the width and depth of wear scratch of CoNi alloy coating is larger, indicating that the wear resistance of CoNi alloy coating is poor. With the increase of sodium hypophosphite concentration from 5 g/L to 15 g/L, the width and depth of the wear scratches

on the surface of CoNiP alloy coatings gradually decrease, showing better wear resistance. When the content of sodium hypophosphite in the bath is greater than 15 g/L, due to the strong reducing performance of sodium hypophosphite, the plating solution is unstable and the surface of the coating is loose and rough, resulting in the increase of the width and depth of wear scratch that contributes to the decline in wear resistance. Sodium hypophosphite is mainly used in electroless plating solutions [45-47]. The reducibility and stability of sodium hypophosphite have also been described in some literatures [48-50].

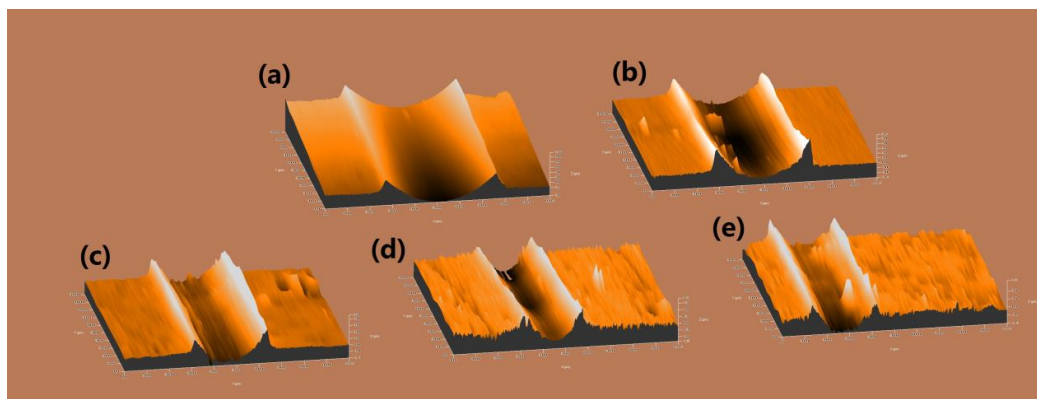


Figure 6. Wear scratch of CoNiP alloy coatings prepared from solutions with different amounts of sodium hypophosphite; a:0 g/L NaH_2PO_2 ; b:5 g/L NaH_2PO_2 ; c:10 g/L NaH_2PO_2 ; d:15 g/L NaH_2PO_2 ; e:20 g/L NaH_2PO_2 ; Middle area ($1000\ \mu\text{m}\times 1000\ \mu\text{m}$) of the wear scratch is scanned to make the profile at the scanning rate of $10\ \mu\text{m/s}$.

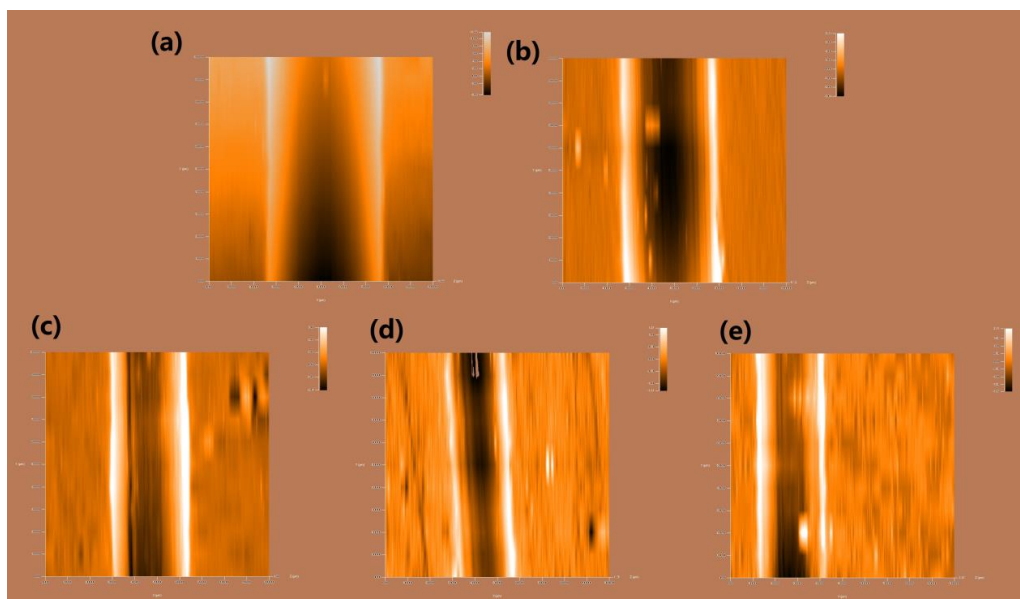


Figure 7. Top view of wear scratch on CoNiP alloy coatings prepared from solutions with different amounts of sodium hypophosphite; a:0 g/L NaH_2PO_2 ; b:5 g/L NaH_2PO_2 ; c:10 g/L NaH_2PO_2 ; d:15 g/L NaH_2PO_2 ; e:20 g/L NaH_2PO_2 ; Middle area ($1000\ \mu\text{m}\times 1000\ \mu\text{m}$) of the wear scratch is scanned to make the profile at the scanning rate of $10\ \mu\text{m/s}$.

In order to accurately measure the geometric parameters of the wear scratches, Figure 7 shows the top view of the wear scratches and the geometric parameters are listed in table 4.

Table 4. Depth and width of wear scratches on CoNiP alloy coatings

Sample	NaH ₂ PO ₂ / g/L	Maximum depth of wear scratch/ μm	Maximum width of wear scratch/ μm
a	0	5.08	542.86
b	5	2.86	428.57
c	10	2.07	328.24
d	15	1.35	257.14
e	20	2.05	314.19

Combined with the data in Figure 7 and Table 4, it can be seen that CoNi alloy coating obtained without phosphorus doping has the worst wear resistance with the deepest wear depth and the largest wear width which are 5.08 μm and 542.86 μm respectively. However, CoNiP alloy coating prepared from bath with 15 g/L sodium phosphite possesses excellent wear resistance with the lowest wear depth and the smallest wear width.

4. CONCLUSIONS

In this paper, CoNiP alloy coatings were electrodeposited on the surface of 42CrMo steel plate as gear material to improve mechanical performance. The effect of sodium hypophosphite concentration on the electrochemical curves, surface morphology, structure, thickness and wear resistance in simulated oil was studied. Phosphorus is precipitated under the catalytic action of cobalt and nickel. Sodium hypophosphite content in the plating solution is beneficial to accelerate the electrochemical reaction, improve the thickness and refine the surface particles of the CoNiP alloy coating resulting in the improvement of wear resistance performance. However, when the content of sodium hypophosphite in the bath is greater than 15 g/L, the plating solution becomes unstable and the surface of the coating is loose and rough, resulting in the decline of wear resistance. The CoNiP alloy coating prepared from bath with 15 g/L sodium hypophosphite possesses excellent wear resistance with the lowest wear depth and the smallest wear width.

ACKNOWLEDGMENTS

This work is supported and funded by education science 13th five-year planning project of Gansu province (GS[2020]GHB4614).

References

1. X. Z. Li, C. S. Song, Y. Yang, C. C. Zhu and D. L. Liao, *Mech. Mach. Theory*, 152 (2020) 103941.

2. B. Haefner and G. Lanza, *CIRP Ann.*, 66 (2017) 475.
3. J. Z. Su, Z. D. Fang and X. W. Cai, *Chin. J. Aeronaut.*, 26 (2013) 1310.
4. F. L. Litvin, I. G. Perez, A. Fuentes and K. Hayasaka, *Comput. Methods Appl. Mech. Eng.*, 197 (2008) 3783.
5. Z. Q. Cai, S. Kang, J. W. Lv, S. Zhang, Z. L. Shi, Y. J. Yang and M. Z. Ma, *J. Non-Cryst. Solids*, 581 (2022) 121428.
6. K. S. Sajal, P. A. Kumarappan, A. J. Kevin, V. S. Sri and R. L. Bhaskara, *Mater. Today: Proc.*, 50 (2022) 2092.
7. A. Rohrmoser, H. Hagenah and M. Merklein, *Procedia Manuf.*, 53 (2021) 189.
8. A. L. Tour, M. Charles, N. Raghunathan and M. Ahlfors, *Int. J. Refract. Met. Hard Mater.*, 91 (2020) 105272.
9. K. Gupta and S. Chatterjee, *Mater. Today: Proc.*, 5 (2018) 789.
10. X. M. Li, M. Sosa, M. Andersson and U. Olofsson, *Tribol. Int.*, 95 (2016) 211.
11. Y. D. Yu, Y. Cao, M. G. Li, G. Y. Wei and H. Dettinger, *Mater. Res. Innovations*, 18 (2014) 314.
12. S. H. Son, S. C. Park, W. Lee and H. K. Lee, *T. Nonferr. Metal Soc.*, 23 (2013) 366.
13. Z. K. Qiu, P. Z. Zhang, D. B. Wei, X. F. Wei and X. H. Chen, *Surf. Coat. Technol.*, 278 (2015) 92.
14. D. Fiquet, A. Billard, C. Savall, J. Creus, S. Cohendoz, J. L. G. Poussard, *Mater. Chem. Phys.*, 276 (2022) 125332.
15. S. K. Ghosh and J. P. Celis, *Tribol. Int.*, 68 (2013) 11.
16. Y. D. Yu, M. G. Li, G. Y. Wei and H. L. Ge, *Surf. Eng.*, 29 (2013) 767.
17. Z. H. Huang, Y. J. Zhou and T. T. Nguyen, *Surf. Coat. Technol.*, 364 (2019) 323.
18. Y. Zhou, F. Q. Xie, X. Q. Wu, W. D. Zhao and X. Chen, *J. Alloys Compd.*, 699 (2017) 366.
19. H. H. Sheu, P. C. Huang, L. C. Tsai and K. H. Hou, *Surf. Coat. Technol.*, 235 (2013) 529.
20. N. K. Shrestha, M. Masuko and T. Saji, *Wear*, 254 (2003) 555.
21. S. Kallel, B. Semmache, M. Lemiti, H. Jaffrezic and A. Laugier, *Microelectron. J.*, 30 (1999) 699.
22. H. Miura, N. Saito and N. Okamoto, *Microelectron. J.*, 26 (1995) 249.
23. F. J. He, H. Su, H. Ju, L. Tan and Q. Zhou, *Surf. Coat. Technol.*, 213 (2012) 133.
24. K. Moon, J. Y. Seo and B. Y. Yoo, *Int. J. Refract. Met. Hard Mater.*, 100 (2021) 105627.
25. K. X. Gao, X. L. Wei, G. Q. Liu, B. Zhang and J. Y. Zhang, *Chem. Phys.*, 537 (2020) 110857.
26. Y. C. Wu, Z. Y. Zhang, K. Xu, J. Z. Lu, A. Wang, X. R. Dai and H. Zhu, *Appl. Surf. Sci.*, 535 (2021) 147707.
27. S. B. Liu, I. Shohji, T. Kobayashi, J. Hirohashi, T. Wake, H. Yamamoto and Y. Kamakoshi, *J. Electroanal. Chem.*, 897 (2021) 115582.
28. M. J. Kim, S. H. Lee, J. G. Kim and J. B. Yoon, *Corros.*, 66 (2010) 125005.
29. Y. R. Wang, X. Y. Cao, Z. M. Wang, Z. D. Chen and N. Mitsuzaki, *Int. J. Electrochem. Sci.*, 14 (2019) 8185.
30. H. Z. Huang, X. Q. Wei, D. Q. Tan and L. Zhou, *Int. J. Miner. Metall. Mater.*, 20 (2013) 563.
31. B. K. Panigrahi, S. Srikanth and G. Sahoo, *J. Mater. Eng. Perform.*, 18 (2009) 1102.
32. K. S. N. Vikrant and S. Allu, *J. Electrochem. Soc.*, 168 (2021) 020536.
33. V. A. Isaev, O. V. Grishenkova and Y. P. Zaykov, *J. Electroanal. Chem.*, 818 (2018) 265.
34. M. P. Pardave, B. R. Scharifker, E. M. Arce and M. R. Romo, *Electrochim. Acta*, 50 (2005) 4736.
35. M. Pise, M. S. Muduli, A. Chatterjee, B. P. Kashyap, R. N. Singh and S. S. V. Tatiparti, *Results Surf. Interfaces*, 6 (2022) 100044.
36. Y. D. Yu, L. X. Sun, H. L. Ge, G. Y. Wei and L. Jiang, *Int. J. Electrochem. Sci.*, 12 (2017) 485.
37. K. Dhanapal, V. Narayanan and A. Stephen, *Mater. Chem. Phys.*, 166 (2015) 153.
38. Y. E. Sknar, O. O. Savchuk and I. V. Sknar, *Appl. Surf. Sci.*, 423 (2017) 340.
39. J. Naderi and A. A. D. Sarhan, *Meas.*, 139 (2019) 490.
40. A. M. Pillai, A. Rajendra and A. K. Sharma, *J. Coat. Technol. Res.*, 9 (2012) 785.
41. S. Thanikaikarasan, T. Mahalingam, T. Ahamad and S. M. Alshehri, *J. Saudi Chem. Soc.*, 24 (2020) 955.

42. P. Cojocaru, L. Magagnin, E. Gomez and E. Valles, *J. Alloys Compd.*, 503 (2010) 454.
43. E. B. Modin, E. V. Pustovalov, A. N. Fedorets, A. V. Dubinets, B. N. Grudin, V. S. Plotnikov and S. S. Grabchikov, *J. Alloys Compd.*, 641 (2015) 139.
44. C. Ma, S. Wang and F. C. Walsh, *Trans. Inst. Met. Finish.*, 93 (2015) 275.
45. F. Z. Yang, B. Yang, B. B. Lu, L. Huang, S. K. Xu and S. M. Zhou, *Acta Phys. Chim. Sin.* 22 (2006) 1317.
46. L. P. Wu, Z. D. Yang and G. W. Qin, *J. Alloys Compd.*, 694 (2017) 1133.
47. L. L. Wei, H. H. Shu and J. C. Wen, *Int. J. Miner. Metall. Mater.*, 16 (2009) 197.
48. Y. J. Chu, G. Yu, B. N. Hu, Q. Z. Dong, J. Zhang and X. Y. Zhang, *Adv. Powder Technol.*, 25 (2014) 477.
49. J. K. Yu, S. Zhai, M. Q. Yu, H. L. Luo, Q. Qiao, J. Zhao, Z. F. Xu and K. Matsugi, *J. Mater. Eng. Perform.*, 26 (2017) 3915.
50. O. Elendu, M. Ojewumi, Y. D. Yeboah and E. E. Kalu, *Int. J. Electrochem. Sci.*, 10 (2015) 10792.

© 2022 The Authors. Published by ESG (www.electrochemsci.org). This article is an open access article distributed under the terms and conditions of the Creative Commons Attribution license (<http://creativecommons.org/licenses/by/4.0/>).